CNPY2 governs PDGF-BB-treated vascular smooth muscle cell proliferation, migration and phenotypic transformation via the Akt/mTOR/GSK-3β signaling pathway

HOUQI SUN[1], XUEJIE WANG[2], LING MA[3], XU LI[4], WENJING JIN[5] and YONGBIN YANG[1]

Departments of [1]Interventional Medicine, [2]Hypertension, [3]General Medicine, [4]General Surgery and [5]Medical Imaging, Bazhou People's Hospital, Korla, Xinjiang 841000, P.R. China

Received August 29, 2023; Accepted January 12, 2024

DOI: 10.3892/etm.2024.12485

Abstract. Phenotype switching of vascular smooth muscle cells (VSMCs) is a pathological process in various vascular diseases. Canopy FGF signaling regulator 2 (CNPY2) has previously been found to be abnormally expressed in ApoE$^{-/-}$ mice and aortic endothelial cells, indicating it may have an important role in vascular diseases. The present study aimed to determine the role and mechanism of CNPY2 in VSMC phenotype switching. Following stimulation with platelet-derived growth factor type BB (PDGF-BB), the expression of CNPY2 in VSMCs was detected using reverse transcription-quantitative PCR and western blot analysis. Subsequently, to explore the regulatory effects of CNPY2 on VSMCs, CNPY2 expression was knocked down by transfection with short hairpin RNA and cell viability, proliferation, migration and phenotypic transformation indicators were detected. Western blot analysis was also used to detect the phosphorylation of Akt/mTOR/GSK-3β pathway-associated proteins downstream of CNPY2. In addition, pretreatment with the Akt pathway activator SC79 was performed to further explore the regulatory mechanisms of CNPY2. The results revealed that CNPY2 expression was upregulated in PDGF-BB-stimulated VSMCs. In addition, the knockdown of CNPY2 inhibited PDGF-BB-induced VSMC hyperproliferation, cell cycle arrest, migration and phenotypic transformation, as well the activation of Akt/mTOR/GSK-3β pathway-associated proteins. Pretreatment with SC79 significantly reversed the inhibitory effects of CNPY2 knockdown on the proliferation, cell cycle arrest, migration and phenotypic transformation of the model cells. In summary, the present study indicates that CNPY2 regulates the abnormal proliferation, migration and phenotypic transformation of PDGF-BB-stimulated VSMCs via activation of the Akt/mTOR/GSK-3β signaling pathway.

Correspondence to: Dr Yongbin Yang, Department of Interventional Medicine, Bazhou People's Hospital, 56 Renmin East Road, Korla, Bayingolin Mongol Autonomous Prefecture, Xinjiang 841000, P.R. China
E-mail: yangyb830428@163.com

Key words: canopy FGF signaling regulator 2, atherosclerotic occlusive disease, proliferation, migration, phenotypic transformation, Akt/mTOR/GSK-3β signaling

Introduction

Atherosclerosis (AS) involves the coronary and peripheral arteries and can have consequences such as ischemia of the lower limbs and myocardium, or chronic heart failure (1). Atherothrombosis represents the terminal manifestation of this pathology. Plaque rupture or erosion and the intimal thickening of blood vessels cause occlusion, which may cause patients to experience claudication, myocardial infarction, stroke and other symptoms (2). Lower extremity atherosclerotic occlusive disease (ASO) is the most common type of peripheral vascular obliterans. ASO has an incidence rate of 12-14% in the global population, and ~200 million individuals worldwide are known to have ASO, which is life-threatening in certain cases (3). The first-line treatments for occlusion are percutaneous transluminal angioplasty and stent placement (4,5); however, in-stent restenosis or intimal hyperplasia after interventional therapy remain a challenge. Therefore, understanding the pathogenesis of occlusion is the focus of current research.

Previous studies have revealed that vascular smooth muscle cell (VSMC) phenotype switching is a pathological process in various vascular diseases, including AS, postoperative restenosis and aneurysms (6-8). Phenotypic regulation is a prerequisite for VSMC proliferation and migration from the capsular media to the arterial wall intima. The major manifestations of this process include the transformation of cells from a contractile (differentiated) to a synthetic (proliferative) phenotype (9). Contractile VSMCs are spindle-shaped and function as arterial elastic constrictors. Smooth muscle cell (SMC)-specific differentiation proteins, such as α-smooth muscle actin, smooth muscle 22α and calmodulin, are the major components that contribute to the contractility of the cells (10). By contrast, the synthetic phenotype is characterized by the reduced expression of SMC-specific markers, increased osteopontin (OPN) expression and transformation to a rhomboid cell morphology, accompanied by increased proliferation

and migration capabilities, and the secretion of extracellular matrix components (11). Additionally, under the action of risk factors, such as high pressure, lipid deposition, inflammation and infection, vascular endothelial structure and function are impaired, which leads to the synthesis and release of vasoactive substances and cytokines (12), particularly platelet-derived growth factor (PDGF). PDGF type BB (PDGF-BB) is one of the first factors discovered to promote the phenotypic transformation of VSMCs (13). PDGF-BB acts on VSMC membrane receptors and activates various intracellular signal transduction pathways, including the Ras/Raf/MEK/ERK, PI3K/Akt, NF-κB and JAK2/STAT3 pathways, thereby producing a dedifferentiation effect (10). In addition, basic fibroblast growth factor and epidermal growth factor are also able to induce VSMC phenotypic transformation (14). Exploring the mechanisms responsible for the abnormal proliferation, migration and phenotypic transformation of VSMCs may provide an effective strategy for the treatment of arterial occlusion.

Canopy FGF signaling regulator 2 (CNPY2) is a cytoplasmic secreted protein that is widely expressed in various tissues and organs, and is a member of the canopy family, which also includes CNPY1, 3 and 4. Recently, it has been demonstrated that CNPY2 is an angiogenic growth factor (15). CNPY2 has also been found to be abnormally highly expressed in $ApoE^{-/-}$ mice and oxidized low-density lipoprotein-stimulated mouse aortic endothelial cells. In the former, it was found to aggravate the atherosclerotic process via the induction of vascular endothelial cell damage through the activation of protein kinase R-like endoplasmic reticulum kinase signaling (16). In addition, the hypoxia response element upstream of the CNPY2 promoter can bind to hypoxia-inducible factor-1α and thereby promote the migration and proliferation of SMCs and tissue angiogenesis when induced by hypoxia (17). Considering that arterial occlusion can lead to chronic hypoxia in the limbs or organs, it is reasonable to hypothesize that CNPY2 is involved in the proliferation, migration and phenotypic transformation of VSMCs.

When platelets come into contact with the injured vessel wall, PDGF is released which drives intimal layer proliferation and leads to occlusion (18). The present study aimed to examine the potential changes in the expression of CNPY2 in response to PDGF, and to determine the effects of CNPY2 on the proliferation, migration and phenotypic transformation of VSMCs, as well as the underlying mechanisms.

Materials and methods

Cells, cell culture and treatments. Human VSMCs (T/G HA-VSMC cell line; passage 2) were purchased from Shanghai Jinyuan Biotechnology Co., Ltd. (cat. no. JY524) and cultured in Dulbecco's modified Eagle's medium (DMEM; Gibco; Thermo Fisher Scientific, Inc.) containing 10% fetal bovine serum (FBS; Gibco; Thermo Fisher Scientific, Inc.) and 100 U/ml penicillin and 0.1 mg/ml streptomycin (Gibco; Thermo Fisher Scientific, Inc.) at 37˚C with 5% CO_2. VSMCs were passaged at 1:2, and passages 3-5 were used for the experiments. A concentration of 20 ng/ml PDGF-BB (MilliporeSigma) was used to stimulate the VSMCs at 37˚C for 24 h. In addition, in certain experiments the cells were pre-treated with the Akt activator SC79 (MilliporeSigma) at 10 μM for 2 h (19).

Reverse transcription-quantitative PCR (RT-qPCR). Total RNA was extracted from the cells using VeZol reagent (cat. no. R411; Vazyme Biotech Co., Ltd.). The HiScript II 1st Strand cDNA synthesis kit (cat. no. R211; Vazyme Biotech Co., Ltd.) was used to reverse transcribe the isolated RNA into cDNA according to the manufacturer's protocols. qPCR was then performed using synthetic primers and AceQ® qPCR SYBR Green Master Mix (cat. no. Q111-02; Vazyme Biotech Co., Ltd.) with a Stepone™ Software v2.3 Detection System (Thermo Fisher Scientific, Inc.). The conditions were 95˚C for 30 sec, and 40 cycles of 95˚C for 5 sec, 55˚C for 10 sec and 72˚C for 15 sec. The mRNA levels of CNPY2 were normalized to those of GAPDH and calculated using the $2^{-\Delta\Delta Cq}$ method (20). The primer sequences (5'-3') were as follows: CNPY2, forward, TAGTGGGCCGGAATGGAGAA and reverse, AAACTT GAGGGTGCCGCTAA; GAPDH, forward, GACTCATGA CCACAGTCCATGC and reverse, AGAGGCAGGGATGAT GTTCTG.

Western blot analysis. Proteins were extracted from the cells ($5x10^6$) using RIPA lysis buffer (Beyotime Institute of Biotechnology). The protein concentration of the extract was determined using a BCA kit (Beyotime Institute of Biotechnology). A total of 30 μl protein/lane was then separated using 10% SDS-PAGE and transferred to PVDF membranes (SEQ00010; MilliporeSigma). After blocking the membranes with bovine serum albumin (BSA; 5%, v/v; Elabscience Co., Ltd.) at room temperature for 2 h, the membranes were incubated overnight at 4˚C with primary antibodies against CNPY2 (PA5-100135; 1:1,000; Invitrogen; Thermo Fisher Scientific, Inc.), OPN (22952-1-AP; 1:2,000; Proteintech), smooth muscle actin (SMA; 14395-1-AP; 1:3,000; Proteintech), F-actin (MA1-80729; 1:500; Invitrogen; Thermo Fisher Scientific, Inc.), phosphorylated (p-)Akt (66444-1-Ig; 1:20,000; Proteintech), Akt (60203-2-Ig; 1:20,000; Proteintech), p-mTOR (67778-1-Ig; 1:5,000; Proteintech), mTOR (28273-1-AP; 1:5,000; Proteintech), p-GSK-3β (67558-1-Ig; 1:5,000; Proteintech), GSK-3β (22104-1-AP; 1:4,000; Proteintech) and GAPDH (PA1-16777; 1:5,000; Invitrogen; Thermo Fisher Scientific, Inc.). The membranes were washed with TBST (0.05% Tween 20), and then incubated for 120 min at room temperature with secondary antibodies (cat. nos. 31460 and 31430; 1:100,000; Invitrogen; Thermo Fisher Scientific, Inc.). Enhanced chemiluminescence Western Blotting Substrate (32109; Pierce; Thermo Fisher Scientific, Inc.) was used to visualize the bands, and the density of the protein bands was semi-quantified using ImageJ software version 1.8.0 (National Institutes of Health).

Cell transfection. To inhibit CNPY2, the two human CNPY2-targeting pRNAT-U6.1/Neo short hairpin RNAs (shRNAs; 1 μg; sh-CNPY2#1 and sh-CNPY2#2; Guangzhou Ribobio Co., Ltd.) were respectively transfected into cells using Lipofectamine 2000® (Invitrogen; Thermo Fisher Scientific, Inc.). Cells transfected with the same plasmid carrying non-targeting shRNAs served as the negative control (sh-NC). Target sequences were as follows: sh-CNPY2#1, CGAACAGATCTTTGTGACCAT; sh-CNPY2#2, CTTTGC AGTAAGCGAACAGAT; and sh-NC, TTCTCCGAACGT GTCACGT. Complexes of Lipofectamine and shRNA in

serum-free DMEM were added to VSMCs at ~70% confluence. Knockdown efficacy was determined 48 h after transfection at 37˚C (21).

Cell Counting Kit-8 (CCK-8) assay. The cells were plated in 96-well plates ($1x10^3$/well) and then subjected to the aforementioned treatments. Then, 100 μl CCK-8 solution (Dojindo Laboratories, Inc.) was added to the cells for 2 h, after which the optical density was measured at 450 nm using a microplate reader (Thermo Fisher Scientific, Inc.).

5-Ethynyl-2'-deoxyuridine (EdU) staining. The cells were plated in six-well plates ($1x10^5$/well) and subjected to treatment. The cells were then incubated at 37˚C in 20 μM EdU solution from an EdU Cell Proliferation Image Kit (cat. no. KTA2030; Abbkine Scientific Co., Ltd.) for 2 h, and fixed in 4% formaldehyde for 30 min at room temperature (22). The cells were permeated by 0.3% Triton X-100 for 10 min and subsequently exposed to reaction solution (Abbkine Scientific Co., Ltd.) for 30 min, followed by DAPI staining (cat. no. E607303; Sangon Biotech Co., Ltd.) for 30 min at room temperature. Images were captured and analyzed using an inverted fluorescence microscope (Axio Observer Z1; Zeiss AG).

Flow cytometry analysis. The cells were plated in six-well plates ($1x10^5$/well) and were then subjected to treatment. The Cell Cycle Assay Kit (cat. no. E-CK-A351; Elabscience Biotechnology, Inc.) was used for analysis of the cell cycle. Cells were harvested after digestion with 0.25% trypsin (Vazyme Biotech Co., Ltd.), and the supernatant was discarded. The cells were washed with ice-cold PBS and collected after centrifugation at 850 x g for 5 min at 4˚C. Precooled 70% ethanol was used to immobilize the cells at 4˚C for 2 h and then the cells were washed with PBS. Subsequently, the cells were incubated with RNase reagent for 30 min at 37˚C and propidium iodide for 30 min at 4˚C in the dark (23). The cell cycle status was then assessed using flow cytometry (BD Bioscience; excitation wavelength 488 nm) and analyzed using FlowJo version 10 software.

Transwell migration assay. The treated VSMCs ($1x10^4$/well) in serum-free DMEM were plated in the upper chambers of 24-well Transwell plates (pore size, 8.0 μm; Corning, Inc.) and the lower chambers were supplemented with 10% FBS in DMEM. Following 24 h of incubation at 37˚C, the cells on the lower surface of the Transwell membranes were fixed with 4% formaldehyde for 20 min and stained with 0.1% crystal violet at 25˚C for 15 min (24). The migratory cells were observed under a light microscope (BX51W; Olympus Corporation).

Wound healing assay. A cell layer of the treated VSMCs were scratched using a pipette tip to form a straight scratch wound. The cell layer was incubated with serum-free DMEM for 24 h. Images of the wound were captured using a light microscope (BX51W; Olympus Corporation) at 0 and 24 h. Cell migration was analyzed using ImageJ software version 1.8.0 (National Institutes of Health).

Immunofluorescence (IF) analysis. The treated cells were fixed with 4% paraformaldehyde at room temperature for 10 min and blocked with 1% BSA (MilliporeSigma) at room temperature for 30 min, followed by overnight incubation with F-actin primary antibody (MA1-80729; 1:20; Invitrogen; Thermo Fisher Scientific, Inc.) at 4˚C, and then incubation with goat anti-mouse Alexa Fluor™ 488 secondary antibody (A-11001; 1:2,000; Invitrogen; Thermo Fisher Scientific, Inc.) at room temperature for 1 h. Cell nuclei were then stained with DAPI for 5 min at room temperature. Six random high-power fields were selected, and images were obtained using a fluorescence microscope (Axio Observer Z1).

Statistical analysis. Data are presented as the mean ± SD (n≥3). Statistically significant differences between experimental parameters among the groups were analyzed using one-way ANOVA followed by Tukey's test or by unpaired Student's t-test using GraphPad Prism Software Version 6.0 (Dotmatics). $P<0.05$ was considered to indicate a statistically significant difference.

Results

Knockdown of CNPY2 inhibits the PDGF-BB-induced proliferation and cell cycle of VSMCs. After stimulation of the VSMCs with PDGF-BB, the expression of CNPY2 was detected using RT-qPCR and western blot analysis. The results revealed that compared with the untreated control group, the expression of CNPY2 in the PDGF-BB-stimulated cells was significantly increased (Fig. 1A). A CNPY2 interference plasmid was then constructed, and the transfection efficacy was detected using RT-qPCR and western blot analysis (Fig. 1B). Since the interference efficiency achieved with sh-CNPY2#2 was stronger than that of sh-CNPY2#1, sh-CNPY2#2 was selected for use in the follow-up experiments and is henceforth referred to as sh-CNPY2. CCK-8 and EdU assays were used to detect cell viability and proliferation, respectively. The results revealed that the viability and proliferative ability of cells in the PDGF-BB group were increased compared with those in the control group. In addition, cell viability and proliferation in the PDGF-BB + sh-CNPY2 group were decreased compared with those in the PDGF-BB + sh-NC group (Fig. 1C and D). Flow cytometric analysis revealed that the number of cells in the G_0/G_1 phase decreased, and that in the S phase increased following stimulation with PDGF-BB, indicating that the cells were proliferating. In the PDGF-BB + sh-CNPY2 group compared with the PDGF-BB + sh-NC group, the number of cells in the G_0/G_1 phase increased, while that of cells in the S phase decreased, indicating that sh-CNPY2 blocked cell proliferation (Fig. 1E and F).

Knockdown of CNPY2 inhibits the PDGF-BB-induced migration and phenotypic transformation of VSMCs. The results of wound healing and Transwell assays revealed that the migratory ability of the VSMCs significantly increased following stimulation with PDGF-BB, and the knockdown of CNPY2 expression significantly attenuated the PDGF-BB-induced migration of the cells (Fig. 2A and B). When observed under a microscope, it was observed that following stimulation with

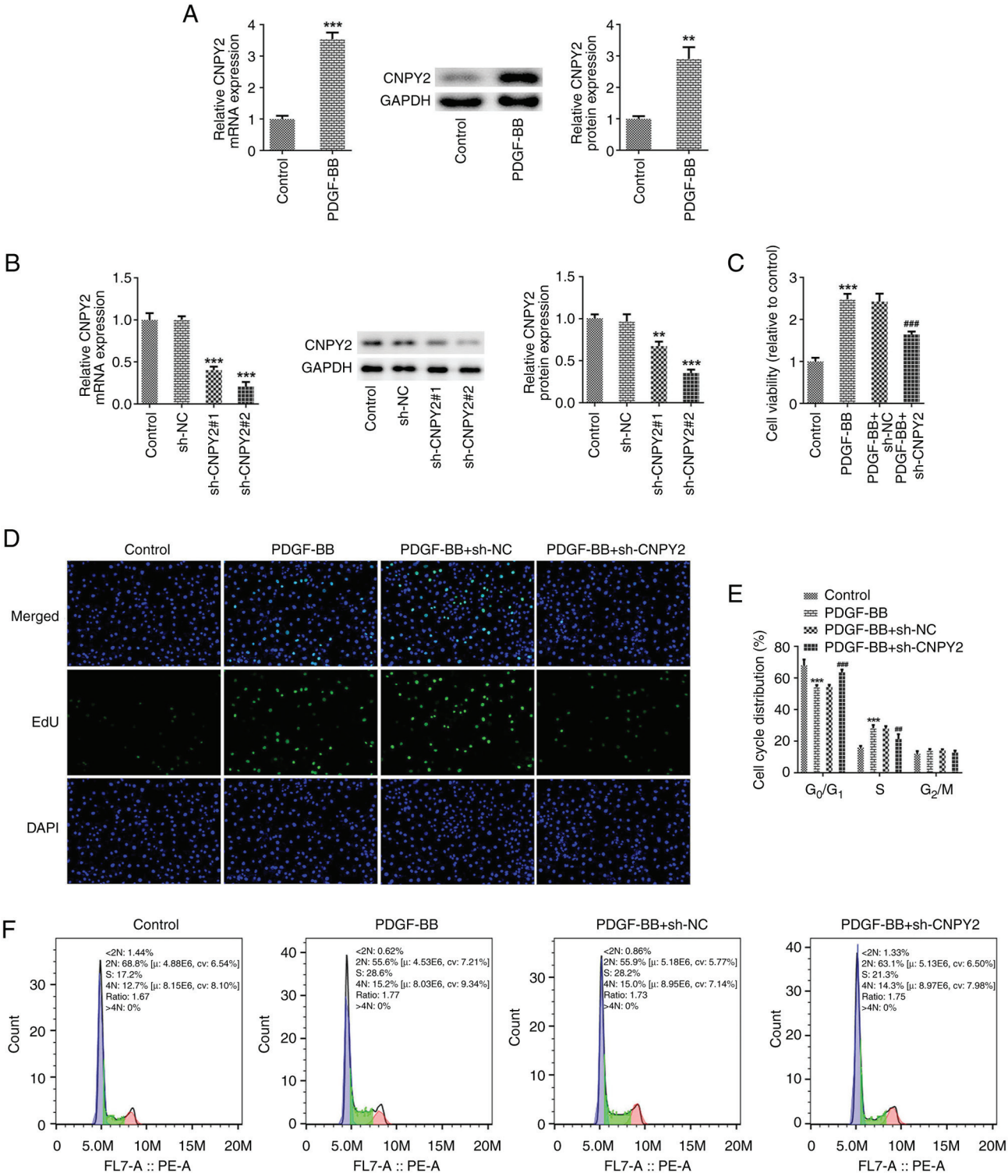

Figure 1. Knockdown of CNPY2 attenuates the PDGF-BB-induced proliferation and cell cycling of VSMCs. (A) Following the stimulation of VSMCs with PDGF-BB, the expression of CNPY2 was detected using RT-qPCR and western blot analysis (n=5). **P<0.01 and ***P<0.001 vs. control. (B) CNPY2 interference plasmids were constructed, and the transfection efficacy was detected using RT-qPCR and western blot analysis (n=5). **P<0.01 and ***P<0.001 vs. sh-NC. (C) Cell Counting Kit-8 assay was used to detect cell viability (n=5). (D) EdU staining was used to detect cell proliferation and representative images are shown (magnification, x200; n=3). (E) Quantification of cell cycle distribution using flow cytometry, and (F) representative flow cytometry plots for the cell cycle analysis (n=5). ***P<0.001 vs. control; $^{\#\#}$P<0.01 and $^{\#\#\#}$P<0.001 vs. PDGF-BB + sh-NC. CNPY2, canopy FGF signaling regulator 2; PDGF-BB, platelet-derived growth factor type BB; VSMCs, vascular smooth muscle cells; RT-qPCR, reverse transcription-quantitative PCR; EdU, 5-ethynyl-2'-deoxyuridine; sh, short hairpin; NC, negative control.

PDGF-BB, the morphology of the VSMCs flattened and the cell bodies increased in size, exhibiting a low degree of differentiation. However, compared with those in the PDGF-BB + sh-NC group, the cell bodies of the PDGF-BB + sh-CNPY2 group were normalized and exhibited a high degree of differentiation (Fig. 2C). The IF staining of cytoskeletal F-actin also showed

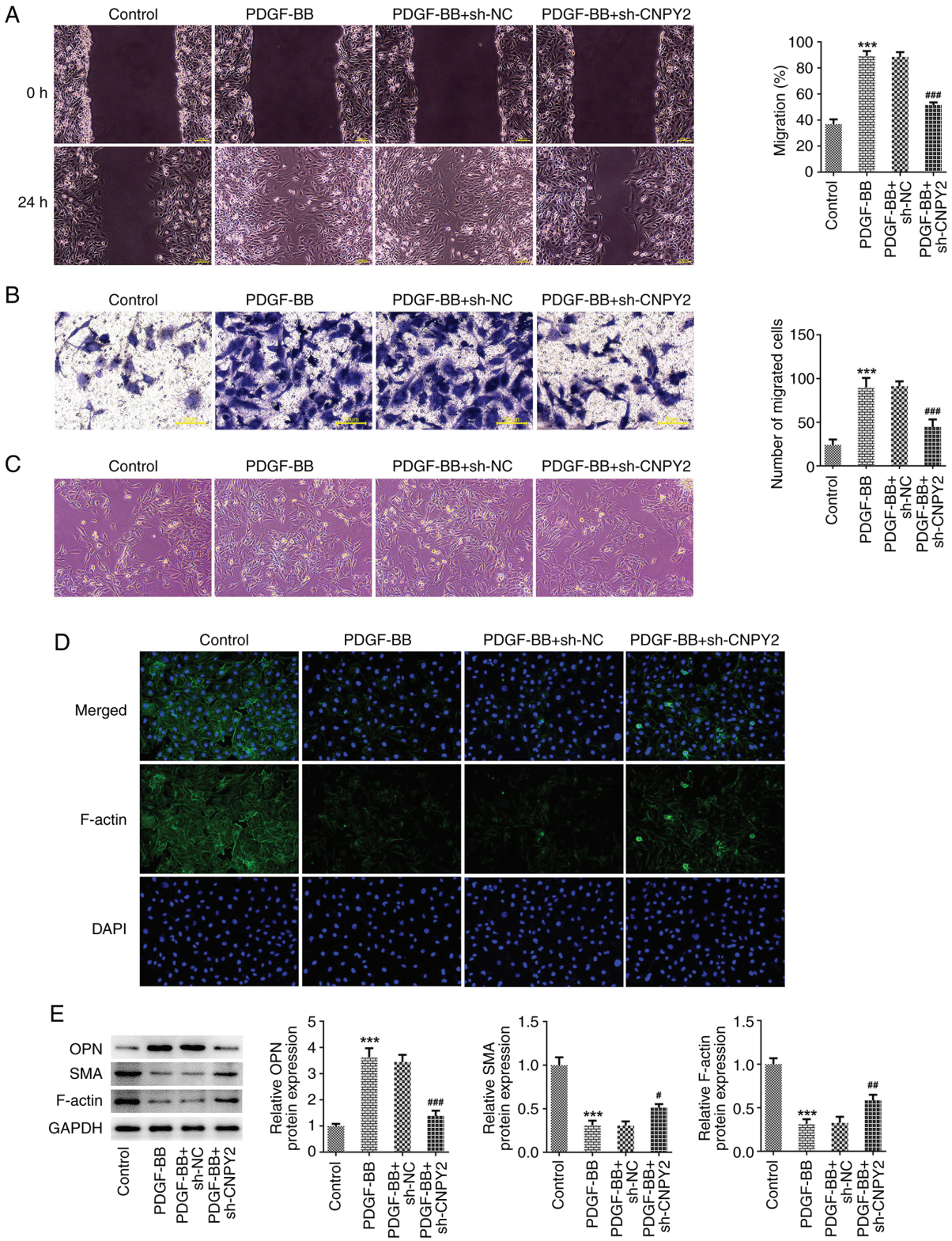

Figure 2. Knockdown of CNPY2 inhibits the PDGF-BB-induced migration and phenotypic transformation of VSMCs. (A) Wound healing (scale bar, 100 μm) and (B) Transwell assays (scale bar, 50 μm) were used to detect the migration ability of the VSMCs (n=3). (C) Images of cell morphology were captured (magnification, x100; n=3). (D) Immunofluorescence staining was used to detect cytoskeletal F-actin (magnification, x200; n=3). (E) Western blot analysis of phenotypic transformation-associated proteins (n=5). ***P<0.001 vs. control; $^{\#}$P<0.05, $^{\#\#}$P<0.01 and $^{\#\#\#}$P<0.001 vs. PDGF-BB + sh-NC. CNPY2, canopy FGF signaling regulator 2; PDGF-BB, platelet-derived growth factor type BB; VSMCs, vascular smooth muscle cells; sh, short hairpin; NC, negative control; OPN, osteopontin; SMA, smooth muscle actin.

that the cell morphology was flattened following stimulation with PDGF-BB, and revealed that the content of myofilaments and structural proteins decreased. However, in comparison with the contents of myofilaments and structural proteins in the PDGF-BB + sh-NC group, those in the PDGF-BB + sh-CNPY2 group were increased (Fig. 2D). Western blot

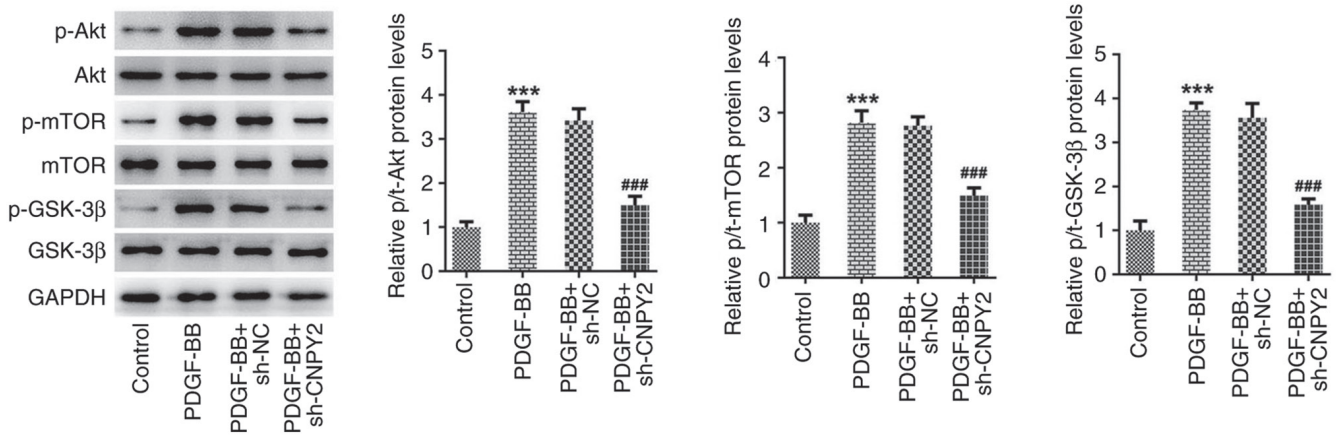

Figure 3. CNPY2 knockdown inhibits activation of the Akt/mTOR/GSK-3β signaling pathway in PDGF-BB-treated vascular smooth muscle cells. Western blot analysis of Akt/mTOR/GSK-3β signaling pathway-associated proteins (n=5). ***P<0.001 vs. control; ###P<0.001 vs. PDGF-BB + sh-NC. CNPY2, canopy FGF signaling regulator 2; PDGF-BB, platelet-derived growth factor type BB; sh, short hairpin; NC, negative control; p-, phosphorylated; t-, total.

analysis demonstrated that in the PDGF-BB group compared with the control group, the expression of OPN was significantly increased, while that of SMA and F-actin was significantly decreased. In addition, in the PDGF-BB + sh-CNPY2 group, OPN expression was significantly decreased while SMA and F-actin expression was significantly increased compared with that in the PDGF-BB + sh-NC group (Fig. 2E).

CNPY2 activates the Akt/mTOR/GSK-3β signaling pathway. Western blot analysis of the proteins in the Akt/mTOR/GSK-3β signaling pathway revealed that the ratios of p-Akt, p-mTOR and p-GSK-3β protein levels to those of the respective total proteins in the cells was significantly increased following stimulation with PDGF-BB. However, the knockdown of CNPY2 expression significantly inhibited the PDGF-BB-induced upregulation of p-Akt, p-mTOR and p-GSK-3β protein levels (Fig. 3).

CNPY2 regulates the PDGF-BB-induced abnormal proliferation, migration and phenotypic transformation of VSMCs via the activation of Akt/mTOR/GSK-3β signaling. To further explore the regulatory mechanisms of CNPY2, the cells were pretreated with the Akt activator SC79. The results of CCK-8 and EdU staining revealed that the cell viability and proliferative capacity of the PDGF-BB + sh-CNPY2 + SC79 group were significantly increased compared with those of the PDGF-BB + sh-CNPY2 group (Fig. 4A and B). Also, flow cytometric analysis demonstrated that the cell cycle and cell proliferation were accelerated in the PDGF-BB + sh-CNPY2 + SC79 group compared with the PDGF-BB + sh-CNPY2 group (Fig. 4C). The results of the wound healing and Transwell assays indicated that the migratory abilities of the VSMCs were significantly increased in the PDGF-BB + sh-CNPY2 + SC79 group compared with the PDGF-BB + sh-CNPY2 group (Fig. 5A and B). In addition, IF staining demonstrated that the content of myofilaments and structural proteins in the PDGF-BB + sh-CNPY2 + SC79 group was reduced compared with that in the PDGF-BB + sh-CNPY2 group (Fig. 5C). Furthermore, western blotting indicated that OPN expression in the PDGF-BB + sh-CNPY2 + SC79 group was significantly increased compared with that in the PDGF-BB + sh-CNPY2 group, while SMA and F-actin expression was significantly decreased (Fig. 5D).

Discussion

In the present study, PDGF-BB was used to stimulate VSMCs in order to explore the regulatory mechanisms of their proliferation, migration and phenotypic transformation. Following its release in response to vascular injury, PDGF-BB serves as a critical stimulating factor and is a major regulator of VSMC growth and proliferation (25). In the present study, following the stimulation of VSMCs by PDGF-BB, it was found that cell viability, proliferation and migration were significantly increased, and phenotypic transformation occurred. Additionally, upregulated CNPY2 expression was observed in PDGF-BB-stimulated VSMCs. Although a previous study has investigated the potential function of CNPY2 in AS, it only found that CNPY2 aggravated oxidized low-density lipoprotein-induced cellular inflammation and apoptosis (16), and did not reveal its pivotal role in VSMC phenotypic switching. Given that VSMC phenotypic switching plays a decisive role in lipoprotein retention, plaque formation and postoperative restenosis (26), elucidation of the role of CNPY2 in VSMC phenotypic switching is important as it highlights the significance of this factor in the pathology of diseases associated with AS. A previous study demonstrated that the proliferation of white blood cells and endothelial cells in CNPY2 knockout mice was significantly less than that in non-knockout mice, resulting in impaired angiogenesis in the mice (27). Furthermore, the study found that endogenous CNPY2 expression was significantly reduced in the cardiac tissue of patients with end-stage heart failure compared with that of control patients. These studies indicate that CNPY2 mediates the maintenance of normal myocardial function and has an active role in repair after cardiac injury. Therefore, in ASO, it is necessary to maintain its level of expression; CNPY2 expression that is too low or too high is not conducive to a healthy vascular environment.

In the present study, after knocking down CNPY2, proteins associated with the downstream Akt/mTOR/GSK-3β signaling

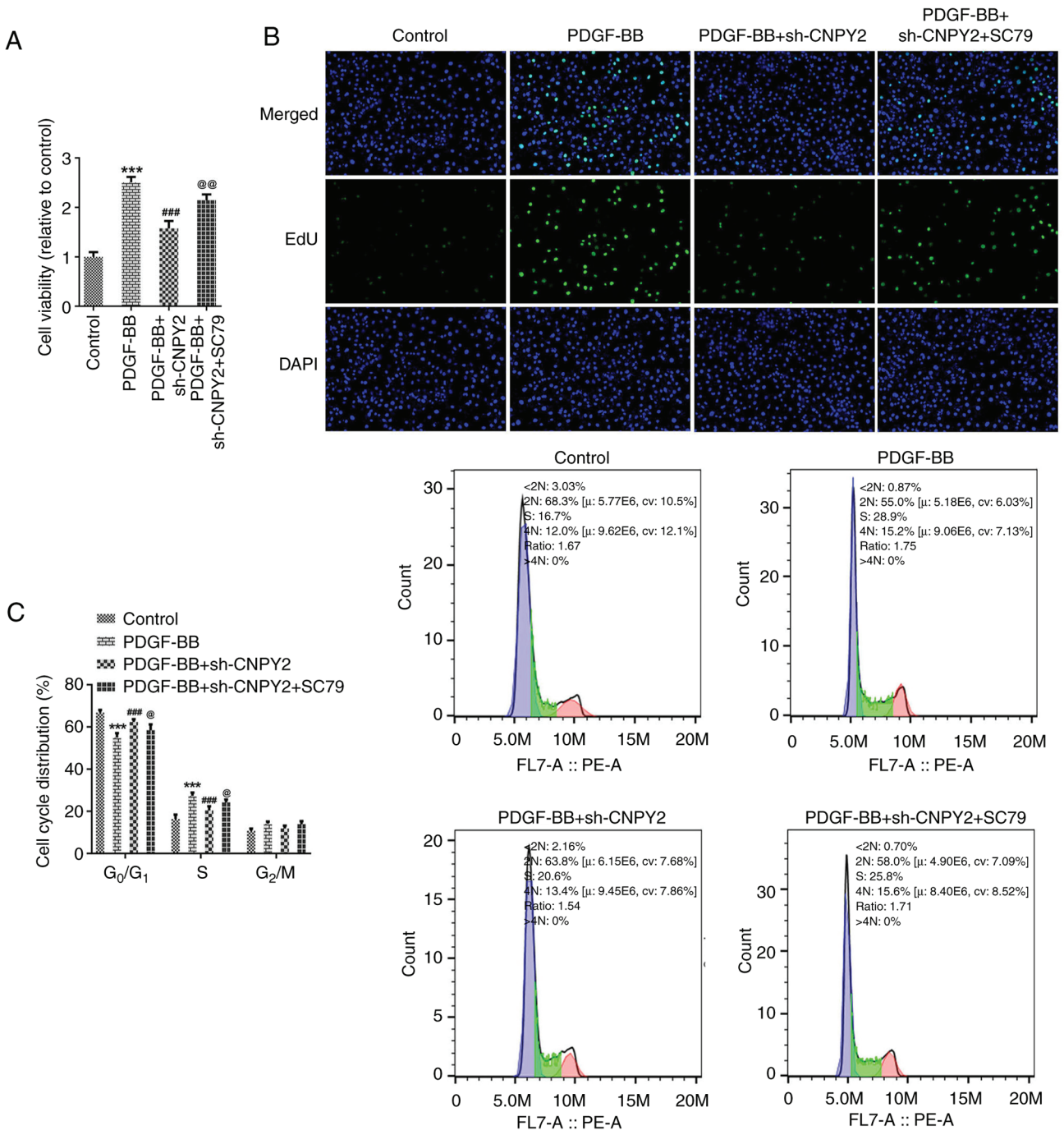

Figure 4. CNPY2 knockdown-induced reductions in the PDGF-BB-induced proliferation and cell cycling of vascular smooth muscle cells are attenuated by activation of the Akt signaling pathway. (A) Cell Counting Kit-8 assay was used to detect cell viability (n=6). (B) EdU staining was used to detect cell proliferation (magnification, x200; n=3). (C) Cell cycle analysis was performed using flow cytometry (n=5). ***P<0.001 vs. control; $^{###}$P<0.001, vs. PDGF-BB; $^{@}$P<0.01 and $^{@@}$P<0.001 vs. PDGF-BB + sh-CNPY2. CNPY2, canopy FGF signaling regulator 2; PDGF-BB, platelet-derived growth factor type BB; EdU, 5-ethynyl-2'-deoxyuridine; sh, short hairpin; SC79, Akt pathway activator.

pathway were evaluated and this signaling pathway was found to be activated. The addition of the Akt signaling pathway activator SC79 significantly attenuated the inhibitory effects of CNPY2 knockdown on PDGF-BB-induced VSMC proliferation, migration and phenotypic transformation. Based on these results, the present study reveals for the first time, to the best of our knowledge, that Akt/mTOR/GSK-3β signaling mediates the regulation of VSMC phenotypic switching by CNPY2. However, previous studies have revealed the regulation of Akt signaling by CNPY2 in other disease models. For example, one study showed that hypoxia-induced CNPY2 promotes the glycolysis of cervical cancer cells via activation of the Akt pathway (28). In another, CNPY2 was shown to enhance epithelial-mesenchymal transformation in non-small cell lung cancer via activation of the Akt/GSK-3β pathway (29). The involvement of Akt signaling in ASO has also been demonstrated, as microRNA-21 was found to be upregulated in the arteries of ASO injury rat models, and was shown to regulate the function of VSMCs through the Akt and ERK1/2 pathways (30). Previous studies have also revealed that Akt

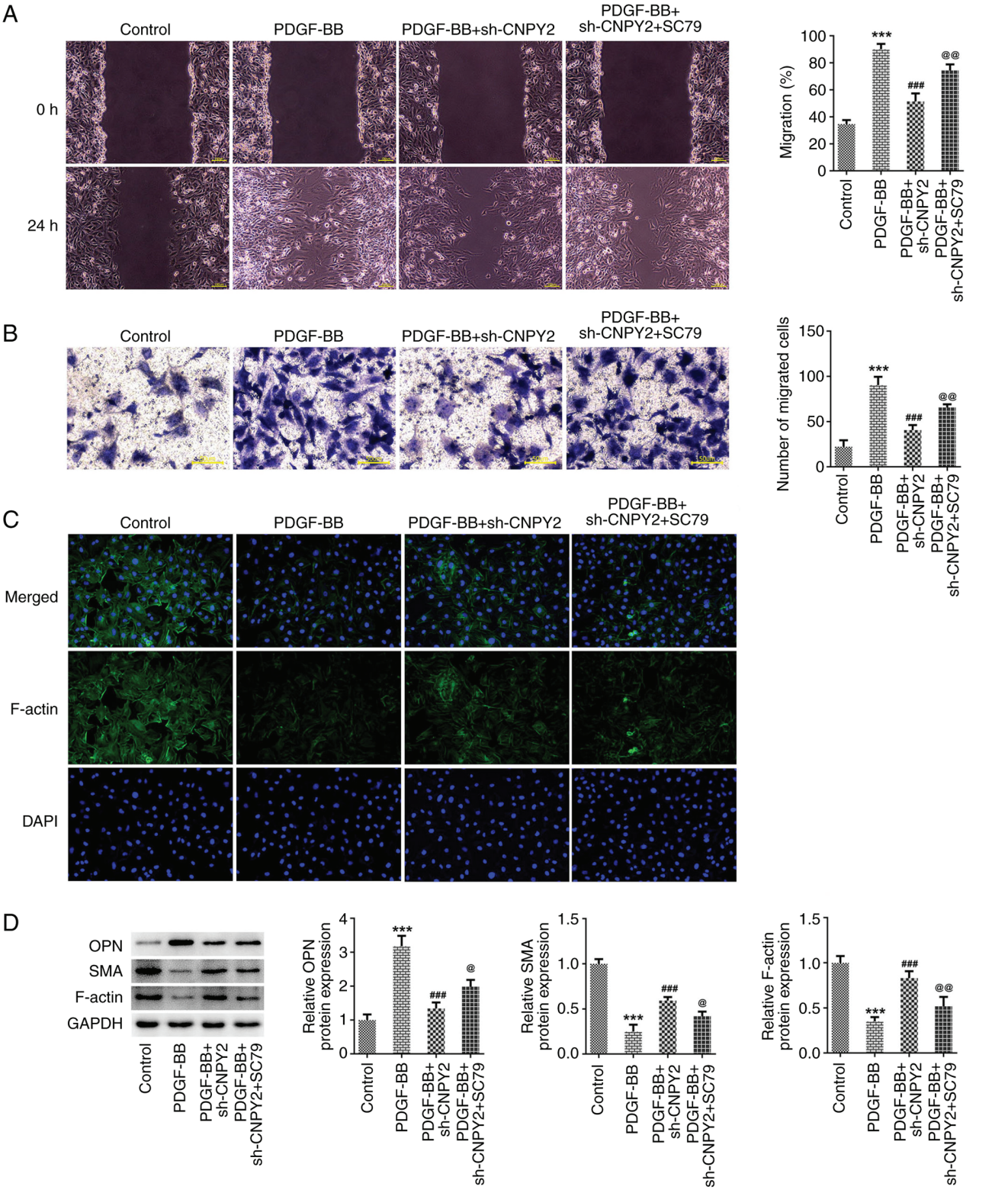

Figure 5. CNPY2 knockdown-induced reductions in the PDGF-BB-induced phenotypic transformation of VSMCs are attenuated by activation of the Akt signaling pathway. (A) Wound healing (scale bar, 100 μm) and (B) Transwell assays (scale bar, 50 μm) were performed to detect the migration ability of the VSMCs. (C) Immunofluorescence staining was used to detect cytoskeletal F-actin (magnification, x200; n=3). (D) Western blot analysis was used to detect the expression of phenotypic transformation-associated proteins (n=5). ***P<0.001 vs. control; $^{###}$P<0.001 vs. PDGF-BB; $^{@}$P<0.01 and $^{@@}$P<0.001 vs. PDGF-BB + sh-CNPY2. CNPY2, canopy FGF signaling regulator 2; PDGF-BB, platelet-derived growth factor type BB; VSMCs, vascular smooth muscle cells; sh, short hairpin; OPN, osteopontin; SMA, smooth muscle actin; SC79, Akt pathway activator.

signaling contributes to the triggering of platelet activation and thrombosis (31,32). The investigation of strategies to block Akt signaling may provide a solution to arterial occlusion. In addition, the discovery of the potential regulatory mechanism of CNPY2 in VSMCs may lead to CNPY2 becoming a disease marker or a target for new therapies.

In conclusion, the present study demonstrates that CNPY2 regulates the abnormal proliferation, migration and phenotypic transformation of PDGF-BB-stimulated VSMCs by activating the Akt/mTOR/GSK-3β signaling pathway. However, this regulatory mechanism of CNPY2 is based on *in vitro* experiments only, and *in vivo* experiments and the analysis of clinical tissues are required to fully uncover its features in the future.

Acknowledgements

Not applicable.

Funding

No funding was received.

Availability of data and materials

The data generated in the present study may be requested from the corresponding author.

Authors' contributions

YY and HS conceived and designed the study. HS, XW, LM, XL and WJ performed the experiments and wrote the manuscript. YY and HS processed the experimental data. YY and HS confirm the authenticity of all the raw data. All authors read and approved the final version of the manuscript.

Ethics approval and consent to participate

Not applicable.

Patient consent for publication

Not applicable.

Competing interests

The authors declare that they have no competing interests.

References

1. Hutchings G, Kruszyna Ł, Nawrocki MJ, Strauss E, Bryl R, Spaczyńska J, Perek B, Jemielity M, Mozdziak P, Kempisty B, *et al*: Molecular mechanisms associated with ROS-dependent angiogenesis in lower extremity artery disease. Antioxidants (Basel 10: 735, 2021.
2. Grover SP and Mackman N: Tissue factor in atherosclerosis and atherothrombosis. Atherosclerosis 307: 80-86, 2020.
3. Zhang R, Lai ZC and Liu CW: Femoral-popliteal arteriosclerosis obliterans:Review of evidence-based studies on drug-eluting endovascular treatment. Zhongguo Yi Xue Ke Xue Yuan Xue Bao 41: 256-260, 2019 (In Chinese).
4. Schicho A, Bäumler W, Verloh N, Beyer LP, Schierling W, Uller W, Gößmann H, Stroszczynski C and Dollinger M: Percutaneous aspiration thrombectomy for arterial thromboembolic occlusion following percutaneous transluminal angioplasty: Technical success rates and clinical outcomes. Rofo 194: 291-295, 2022.
5. Machado M, Borges de Almeida G, Sequeira M, Pedro F, Fior A, Carvalho R, Fragata I, Reis J and Nunes AP: Percutaneous transluminal angioplasty and stenting in acute stroke caused by basilar artery steno-occlusive disease: The experience of a single stroke centre. Interv Neuroradiol 28: 547-555, 2022.
6. Cao G, Xuan X, Hu J, Zhang R, Jin H and Dong H: How vascular smooth muscle cell phenotype switching contributes to vascular disease. Cell Commun Signal 20: 180, 2022.
7. Petsophonsakul P, Furmanik M, Forsythe R, Dweck M, Schurink GW, Natour E, Reutelingsperger C, Jacobs M, Mees B and Schurgers L: Role of vascular smooth muscle cell phenotypic switching and calcification in aortic aneurysm formation. Arterioscler Thromb Vasc Biol 39: 1351-1368, 2019.
8. Zhang L, Tao Y, Yang R, Hu Q, Jia J, Yu M, He B, Shen Z, Qin H, Yu Z and Chen P: Euonymine inhibits in-stent restenosis through enhancing contractile phenotype of vascular smooth muscle cells via modulating the PTEN/AKT/mTOR signaling pathway. Phytomedicine 107: 154450, 2022.
9. Green ID, Liu R and Wong JJL: The expanding role of alternative splicing in vascular smooth muscle cell plasticity. Int J Mol Sci 22: 10213, 2021.
10. Zhang F, Guo X, Xia Y and Mao L: An update on the phenotypic switching of vascular smooth muscle cells in the pathogenesis of atherosclerosis. Cell Mol Life Sci 79: 6, 2021.
11. Wang G, Luo Y, Gao X, Liang Y, Yang F, Wu J, Fang D and Luo M: MicroRNA regulation of phenotypic transformations in vascular smooth muscle: Relevance to vascular remodeling. Cell Mol Life Sci 80: 144, 2023.
12. Medrano-Bosch M, Simón-Codina B, Jiménez W, Edelman ER and Melgar-Lesmes P: Monocyte-endothelial cell interactions in vascular and tissue remodeling. Front Immunol 14: 1196033, 2023.
13. Holycross BJ, Blank RS, Thompson MM, Peach MJ and Owens GK: Platelet-derived growth factor-BB-induced suppression of smooth muscle cell differentiation. Circ Res 71: 1525-1532, 1992.
14. Chen PY, Qin L, Li G, Tellides G and Simons M: Fibroblast growth factor (FGF) signaling regulates transforming growth factor beta (TGFβ)-dependent smooth muscle cell phenotype modulation. Sci Rep 6: 33407, 2016.
15. Chen KQ, Zhang YQ, Wang ZB and Wang SZ: Progress in research on CNPY2 in diseases. Mini Rev Med Chem 24: 391-402, 2024.
16. Huang H, Tang N, Li Y, Huo Q, Chen Q and Meng Q: The role of CNPY2 in endothelial injury and inflammation during the progress of atherosclerosis. J Mol Histol 54: 195-205, 2023.
17. Guo J, Zhang Y, Mihic A, Li SH, Sun Z, Shao Z, Wu J, Weisel RD and Li RK: A secreted protein (Canopy 2, CNPY2) enhances angiogenesis and promotes smooth muscle cell migration and proliferation. Cardiovasc Res 105: 383-393, 2015.
18. Weyand CM and Goronzy JJ: Pathogenic mechanisms in giant cell arteritis. Cleve Clin J Med 69 (Suppl 2): SII28-SII32, 2002.
19. Xu TY, Qing SL, Zhao JX, Song J, Miao ZW, Li JX, Yang FY, Zhao HY, Zheng SL, Li ZY, *et al*: Metrnl deficiency retards skin wound healing in mice by inhibiting AKT/eNOS signaling and angiogenesis. Acta Pharmacol Sin 44: 1790-1800, 2023.
20. Livak KJ and Schmittgen TD: Analysis of relative gene expression data using real-time quantitative PCR and the 2(-Delta Delta C(T)) method. Methods 25: 402-408, 2001.
21. Zhao MJ, Jiang HR, Sun JW, Wang ZA, Hu B, Zhu CR, Yin XH, Chen MM, Ma XC, Zhao WD and Luan ZG: Roles of RAGE/ROCK1 pathway in HMGB1-induced early changes in barrier permeability of human pulmonary microvascular endothelial cell. Front Immunol 12: 697071, 2021.
22. Zhou J, Jiang YY, Chen H, Wu YC and Zhang L: Tanshinone I attenuates the malignant biological properties of ovarian cancer by inducing apoptosis and autophagy via the inactivation of PI3K/AKT/mTOR pathway. Cell Prolif 53: e12739, 2020.
23. Gao Q, Chen K, Gao L, Zheng Y and Yang YG: Thrombospondin-1 signaling through CD47 inhibits cell cycle progression and induces senescence in endothelial cells. Cell Death Dis 7: e2368, 2016.
24. Zhang Q, Lu S, Li T, Yu L, Zhang Y, Zeng H, Qian X, Bi J and Lin Y: ACE2 inhibits breast cancer angiogenesis via suppressing the VEGFa/VEGFR2/ERK pathway. J Exp Clin Cancer Res 38: 173, 2019.
25. Salabei JK, Cummins TD, Singh M, Jones SP, Bhatnagar A and Hill BG: PDGF-mediated autophagy regulates vascular smooth muscle cell phenotype and resistance to oxidative stress. Biochem J 451: 375-388, 2013.
26. Liu YX, Yuan PZ, Wu JH and Hu B: Lipid accumulation and novel insight into vascular smooth muscle cells in atherosclerosis. J Mol Med (Berl) 99: 1511-1526, 2021.

27. Yin W, Guo J, Zhang C, Alibhai FJ, Li SH, Billia P, Wu J, Yau TM, Weisel RD and Li RK: Knockout of canopy 2 activates p16^{INK4a} pathway to impair cardiac repair. J Mol Cell Cardiol 132: 36-48, 2019.
28. Tian T, Dong Y, Zhu Y, Chen Y, Li X, Kuang Q, Liu X, Li P, Li J and Zhou L: Hypoxia-induced CNPY2 upregulation promotes glycolysis in cervical cancer through activation of AKT pathway. Biochem Biophys Res Commun 551: 63-70, 2021.
29. Dou Y, Lei JQ, Guo SL, Zhao D, Yue HM and Yu Q: The CNPY2 enhances epithelial-mesenchymal transition via activating the AKT/GSK3β pathway in non-small cell lung cancer. Cell Biol Int 42: 959-964, 2018.
30. Huang S, Xu T, Huang X, Li S, Qin W, Chen W and Zhang Z: miR-21 regulates vascular smooth muscle cell function in arteriosclerosis obliterans of lower extremities through AKT and ERK1/2 pathways. Arch Med Sci 15: 1490-1497, 2019.
31. Dong J, Lin J, Wang B, He S, Wu C, Kushwaha KK, Mohabeer N, Su Y, Fang H, Huang K and Li D: Inflammatory cytokine TSLP stimulates platelet secretion and potentiates platelet aggregation via a TSLPR-dependent PI3K/Akt signaling pathway. Cell Physiol Biochem 35: 160-174, 2015.
32. Tang Z, Shi H, Chen C, Teng J, Dai J, Ouyang X, Liu H, Hu Q, Cheng X, Ye J, *et al*: Activation of platelet mTORC2/Akt pathway by anti-β2GP1 antibody promotes thrombosis in antiphospholipid syndrome. Arterioscler Thromb Vasc Biol 43: 1818-1832, 2023.